2005

On the Development of a Scalable 8-DoF Model of a Generic Parafoil-Based Delivery System

Yakimenko, Oleg

Monterey, California: Naval Postgraduate School

Yakimenko, O., On the Development of a Scalable 8-DoF Model of a Generic Parafoil-Based Delivery System, Proceedings of the 18th AIAA Aerodynamic Decelerator Systems Technology Conference and Seminar, Munich, Germany, May 23-26, 2005.

https://hdl.handle.net/10945/35325

On the Development of a Scalable 8-DoF Model for a Generic Parafoil-Payload Delivery System

Oleg A. Yakimenko*
Naval Postgraduate School, Monterey, CA 93943-5146

The paper presents an initial move to develop a scalable high-degree-of-freedom model of the parafoil-payload system. The intention is to develop the tool capable of: i) determining basic system's geometry parameters by observing the video data of the real descend, ii) readjusting the nominal aerodynamic and control coefficients incorporated into the well-established equations of motions, and iii) performing model identification to tune numerous relative variables to achieve the best fit with the real drop data if available. Since in the certain way such a tool would represent some kind of generalization of the modeling efforts undertaken so far, the present paper starts from a comprehensive review of publications devoted to the modeling of parafoil-payload systems. The paper then briefly addressed the current stage of the development of a scalable model. In anticipation of real drop data to validate the approach paper ends with conclusions.

I. Introduction

DUE to their ability to cover large horizontal distances from the drop point and their controllability, gliding parachutes offer considerable scope for military application in the delivery of troops, stores and munitions, enhanced safety for aircrew, etc. One concept in the gliding-parachute category which has received attention in mid 60's is a ram-air-inflated fabric wing (called the Jalbert load-distributing flares parafoil). It has a rectangular planform and an airfoil cross-section with an opening at the leading edge to allow ram air to enter and inflate the wing to the desired shape. The payload is suspended on lines below the wing. Some of the earliest projects involving the usage of parafoil-based systems were discussed by Nikolaides and Knapp.[1-7] Lingard[8] provided comprehensive bibliography of ram-air literature up to 1980. Some definitions that in a quarter of a century have become sort of standard, discussion on modern parafoil parameters and their design were presented by Poynter.[9] For the past 40 years a lot of models of different parafoil-payload systems were developed to address the variety of issues. Lately, the high-fidelity 8 and 9 degrees-of freedom (DoF) models were also created.

This paper describes current status of an attempt to develop a scalable model of a generic parafoil-payload system based on the model that has already been developed earlier for the Pegasus payload delivery system by FXC Corp.[10] In what follows the extensive review of the aerodynamic data available for different parafoils as well as numerous attempts to model parafoil-payload systems are given first. Then a brief description of the software developed so far is presented. This tool also employs the system identification tools to better match the real drop data if available. These tools however are considered in a separate paper.[11]

II. Historic Background

A. Wind-Tunnel Tests

Since mid 60's when ram-air parafoils were first introduced many studies have been carried out to establish their basic aerodynamic performance, range of stability and optimal design, to develop relevant models and recently control laws and instrumentation for autonomous payload delivery were addressed. The design of ram-air gliding parachute canopies employs more airplane principles than parachute technology therefore the designers employ texts on basic aerodynamics. One problem that will be encountered is that most airplanes do not fly as slowly as the ram-air canopy (20-25*mph*). Consequently, very little has been done in this area and the information one seeks is usually off the charts. Therefore in what follows we present an overview of different efforts on modeling (in total, over a hundred conference papers, technical reports and journal publications have been collected and reviewed) and we start from the review of experimental data available.

* Research Associate Professor, Dept. of Mechanical and Astronautical Engineering, Code MAE/Yk (oayakime@nps.edu), Associate Fellow AIAA.

The first preliminary wind-tunnel tests and free-flight tests on this type of wing were carried out in wind tunnel of university of Notre Dame by Nikolaides *et al.* in 1964.[1,2] Burk *et al.* presented an investigation of the low-speed static aerodynamic characteristics of three ram-air-inflated low-aspect-ratio parafoils (0.64, 0.78 and 0.94 respectively) in the NASA Langley Research Center full-scale wind tunnel.[12] The aerodynamic coefficients included lift C_L, drag C_D and side-force C_Y coefficients; rolling C_l, pitching C_m and yawing C_n moment coefficients; effective-dihedral $C_{l\beta}$, directional stability $C_{n\beta}$ and side-force parameters $C_{Y\beta}$. The moment reference center was located 4.0 percent of the wing chord aft of the leading edge of the wing and 123 percent of the wing chord below the lower surface of the wing. The results indicated that the untrimmed maximum lift-drag ratios of the wings ranged from 1.9 to 2.7 and that the untrimmed maximum lift coefficients varied from about 0.9 to 1.1. The results of tests of two of the wings selected for a study of their stability characteristics indicated that they were statically longitudinally stable over the entire test angle-of-attack range of 0° to 70°. Both of these wings also had generally satisfactory static lateral stability characteristics over the entire test angle-of-attack range.

Ware *et al.* extended previous results to 11 new models with higher aspect ratios from 1.0 to 3.0.[13] Lift-drag ratio for the constant-area series was reported to be about 2.5 for all aspect ratios (about the same as for a full-scale version), and the maximum lift-drag ratio for the constant chord series varied from 2.2 to 3.3 with increasing aspect ratio. It was also noted that for the wing alone (without suspension lines the lift-drag ration was in average of one unit higher). The data which contained the same list of parameters plus profile-drag C_{D0} and induced-drag C_{Di} coefficients, was referred to the wind system of axes and based on the laid-out-flat wing area and chord of span. The moment reference was the confluence point of the suspension lines, and the one used in stability and control tests was either the 25-percent chord of the lower surface of the wing or an analytically determined center of gravity located 1.5 spans below the wing and positioned longitudinally so as to trim the configuration at the maximum value of lift-drag ratio.

Numerous parafoil configurations which included variations in aspect ratio (0.5 to 3.0), airfoil thickness (0.126 to 0.201), airfoil shape, pennant design, leading edge opening, control surface (flaps) deflections et al. were tested by Nikolaides.[1,5] Also, tests were carried out for a wide range of parafoil size, wind tunnel velocity, and rigging. The list of parameters was broadened to include lift-curve slope $C_{L\alpha}$, pitching stability parameter $C_{m\alpha}$; pitch damping C_{mq} and lag moment $C_{\dot{\alpha}}$ coefficients; drag coefficient of lines $C_{D\pi}$ (which cause as much as 35% of the parasitic drag). Data from various wind tunnel testing programs has been reduced to a common basis and numerous comparison plots illustrating effects of aspect ratio, velocity, trim angle, control deflection and configuration have been presented (see also Ref.2 where the results of the real drops compared to that of experimental prediction are given).

This experimental research confirmed that parafoil is similar to airplane wing. It has positive lift at zero angle of attack and shows lift down to about -5°. The lift curve is quite linear with angle of attack. Increasing the aspect ratio increases the lift curve slope and improves the lift to drag ratio. The parafoil happens to have static and dynamic stability in all modes of flight in pitch, yaw, and roll. Because of its configuration and flexibility, it does not exhibit the stall characteristics of the aeroplane wing at large angles of attack. Instead the lift falls off gently and thus the parafoil may also be safely flown at very large angles of attack (70°+).

These wind tunnel investigations conducted in the 1960's in the University of Notre Dame 2'x2' test section and in the NASA Langley Research Center 30'x60' (elliptic) test section were conducted on models at relatively low wing loadings (1-2lb/ft^2) and small size models up to 300ft^2. They constitute the majority of the experimental data available for small (personnel size) systems. Going beyond the personnel sized canopies (175 to 340ft^2), some very limited research has been done on ram air inflation systems up to 3,200ft^2.

Since the ram-air inflated wing has many proved advantages over the more conventional Parachute system such as low weight, high maneuverability and capability to flare for a soft, stable landing, in late 80's Pioneer Aerospace Corporation chose it for the Advanced Recovery Systems (ARS) for the Next Generation Space Transportation System.[14,15] The canopy size required for this test program must go far beyond any that have been previously studied. The full scale prototype (10,800ft^2, 5.56lb/ft^2) exceeds the size of 3,200ft^2 by 338%. Due to the lack of data for large-size parafoils a large scale wind tunnel tests in the NASA Ames Research Center 80'x120' test section of the National Full-scale Aerodynamic Complex at Moffett Field, California were conducted to establish a data base of large (1,200ft^2) ram air inflated wings.[16] Two models were tested during this investigation - the primary test article, a 1/9 geometric scale model with wing area of 1,200ft^2 and secondary test article, a 1/36 geometric scale model with wing area of 300ft^2, both of which had an aspect ratio of 3.0. The test results showed that large size models were statically stable about a model reference point at angles of attack from 2 to 10 degrees. The maximum

lift-drag ratio varied between 2.9 and 2.4 for increasing wing loading. (The flight test results of the developed full-scale X-38 system were discussed in details nine years later by Iacomimi *et al.*, Martin, Madsen and Cerimele.[17-23])

B. First Modeling Efforts

To this point all aforementioned research provided the only experimental data available to develop different models. Based on this data Lingard applied low aspect ratio wing theory to establish a model from which the glide performance of the most successful gliding parachute, the ram-air, may be understood.[24,8] His predictions were shown to compare well with experiment. Optimum performance for a conventional ram-air parachute was shown to be close to 3:1, the value obtained in practice. Improvements in aerodynamic efficiency with increasing aspect ratio were shown to be largely negated by increased line drag. Optimum aspect ratio and line length were defined. Gliding efficiency was shown to be strongly influenced by the position of the suspended load under the canopy and the ideal location was discussed.

Goodrick used a 3-DoF model to analyze both static and dynamic longitudinal stability of high-performance gliding airdrop systems (parafoils).[25] He also presented results of a 6-DoF simulation and its comparison with the real drop (although equations of motion were omitted).[26,27]

Lingard first derived equations of motion (EoM) of gliding parachute system by resolving the forces horizontally and vertically giving relationships for total horizontal and vertical velocities.[8] These relationships were to be numerically integrated to calculate two-dimensional flight trajectories. It accommodates atmospheric wind effect also. Lingard used this model to study the effect of wind on range covered by the system. Next, two-dimensional 3-DoF dynamic model was developed which was defined by translational velocity components and the angular pitching component. This model was capable of simulating effect on flight dynamics of changes in canopy size, line length, rigging and store mass, and drag along with changes in wind conditions. It was shown that improvements in performance were most likely from drag reduction with useful gains from bi-furcating and minimizing the diameter of suspension lines. However, the greatest gains might be achieved by closing the leading edge of the parachute which in turn necessitates sweeping the wing to maintain the inflated shape. Glide ratios of 6:1 were predicted, doubling the glide ratio of existing systems.

Crimi used a 3-DoF model (lateral channel only) to determine the relationship of aerodynamic and inertial parameters to lateral stability characteristics.[28] He represented the system by a rigid wing with a suspended payload in a steady glide and analytically prescribed stability boundary for spiral divergence. His calculations showed that there is a minimum effective anhedral angle required for absolute stability. Increasing suspension line length is stabilizing for spiral divergence, whereas increasing the glide slope is stabilizing for both spiral divergence and oscillatory response. Iosilevskii used a 3-DoF model (longitudinal channel only) to establish center of gravity and lift coefficient limits for a gliding personal parachute.[29]

Jann discussed two different mathematical models which described the real parafoil-payload system.[30] One was a 3-DoF model and another was a 4-DoF model. In 3-DoF model, only the motion of center of mass is considered. Also, steady state longitudinal motion and no dynamic effect on lateral motion were considered. The 4-DoF model also took the roll angle into account.

Machin *et al.* developed and thoroughly investigated low-order degree of freedom models for longitudinal and lateral channels (separately) of the large-scale ARS (X-38) for the space station crew recovery vehicle.[22] They presented a method of extracting system longitudinal and lateral-directional aero data to feed these models. These data/models were further applied to a NASA Johnson Space Center 8-DoF simulator to receive a reasonable dynamic response match between simulations and flight-test data.[31]

Prakash considered longitudinal stability of the parafoil text vehicle ALEX and basically used one degree of freedom model.[32]

C. Advanced Modeling

Being a very light structure parafoil is strongly influenced by the apparent mass effects of the surrounding air.[8,33] The majority of aforementioned models did not take it in account until this subject was discussed by Lissaman and Brown, who modeled the parafoil as an ellipsoid.[34] Brown provided a discussion of the increasing effect of apparent mass on parafoil turning performance as the scale gets larger.[35] Thomasson derived a new formulation of the EoM of a rigid body in a moving fluid medium which might have velocity gradients or accelerations.[36] He separated out the inertia, apparent mass, and relative velocity effect from derived EoM. Using these EoM, he revealed sources of error in existing parafoil model using classic perfect fluid result. Thus, the formulation provided a common set of EoM for describing the motion of underwater vehicles, airships, parafoils, and airplanes.

Almost all studies of apparent mass effects focused on an ellipsoid, a two-dimensional shape, or an axisymmetric body. An ellipsoid enjoys the virtue of having three planes of symmetry and a geometric centroid that is at the intersection of all three planes. A single center of apparent mass can, therefore, be found that is, not surprisingly, at the centroid. Similarly, when there is axisymmetry, the center of apparent mass must lie along the centerline, and it turns out that in this case a single apparent mass center can also be found that is at the volumetric centroid. In the more general case, it may not be possible to find a single point at which the rotational and translational motions are decoupled.

Barrows examined the case in which there are only two planes of symmetry, such that the parafoil has lateral symmetry and fore-and-aft symmetry, but the top half is not the same as the bottom half.[37,38] Therefore, for each of the three axes of motion, what we have been calling the center must lie somewhere on the intersection of the two planes of symmetry, but they may not coincide allowing for more than one center of apparent mass. Barrows computed the apparent mass of a parafoil shape for motions along various axes using potential flow analysis (no account has been taken of the manner in which the presence of vortices may alter the kinetic energy of the flow). From this, the 6x6 apparent mass matrix about some reference point was derived and parametric forms for estimating the terms of this matrix were suggested. The existence of multiple mass centers results in off-diagonal terms in this matrix that couple the translational and rotational motions. A fully populated apparent inertia matrix has 36 terms, of which only 21 are distinct because it must be symmetric. If the body has both lateral and fore-and-aft symmetry, there are only eight fundamental parameters of apparent inertia. Barrows has shown how the non-diagonal 6x6 apparent inertia matrix about a certain reference point can be used to compute the corresponding apparent mass matrix at any other reference point. He also presented dynamic EoM including nonlinear terms.

Barrows noticed that whoever stated that a little bit of knowledge is a dangerous thing could have had apparent mass in mind. As an example he presents comparison of parachute roll motions about a point near the confluence point of the suspension lines. He showed that the effect of the apparent roll inertia may be greatly reduced by spanwise camber. Lissaman and Brown, using a wing model with no spanwise camber (a flat wing), concluded that the apparent roll inertia may be as much as five times the solid mass roll inertia.[34] The analysis by Barrows concluded that roll inertia of a cambered wing about the roll center may be as small as 0.1 of the corresponding value for a flat wing. The result is that the roll acceleration is much greater than expected from a flat-wing model. Steady-state turn rates may also be altered when compared to the flat-wing results, but not as dramatically.

For a long time 2- DoF or 3-DoF models were the only models needed to analyze/optimize the integral behavior and design of parafoils. Then, the need for a higher fidelity models emerged to study the behavior parachute-submunition systems and recently to support autonomous control system development. Some of the on autonomous delivery system design projects are the Automatically Guided Parafoil, by European Space Agency (1997), Small Autonomous Parafoil Landing Experiment ALEX by Institute of Flight Mechanics of the German Aerospace Center (1999),[39,40] High Altitude Balloon Experiments in Technology HABET by Iowa State University,[41] Automatic Parafoil by RIEGL (2000), Advanced Precision Aerial Delivery System by FXC Corporation (2001),[42] Precision Guided Parachute System by Atair Aerospace (2003) and others. Obviously for more sophisticated models the coefficients provided by the experimental research were not sufficient. That's where Prandtl lifting line theory and computational fluid dynamics (CFD) methods helped evaluate missing coefficients.[43-48] For instance, Brown[35] used scalar aerodynamic coefficients calculated using discrete vortex Weissinger method (extended lifting line theory) by Kroo.[49] (It should be noted that while the coefficients provided by wind-tunnel experiments are know within the wide range of angle of attack and side-slip angle the coefficients supplied by CFD are usually just static scalars.)

Detailed dynamic simulation of the flight mechanics of parachute (or parafoil[*]) and payload systems (two bodies having a specific joint at the confluence point) appears to have commenced in 1968 with PhD work of Wolf, who considered the stability of a parachute connected to a load.[50] Pillasch and Shen concluded that, 6-DoF model, useful for rigid body dynamics, is inadequate for the flight dynamics of the parachute-submunition system, therefore it requires more degrees of freedom.[51] They reported that for the three-body parachute submunition including a friction plate and elastic suspension lines they developed two versions of the enhanced model: 10-DoF and 15-DoF (it our opinion that here and in some other publications degrees of freedom for multiple-body systems are not being counted properly but we leave as it was reported in the reference and will discuss it in the following subsection). They also provided Lagrangian equations and some details on the first one, 10-DoF model. In 1987 Reif published another 9-DoF model and simulation results which compared well with measured oscillations of a parachute-payload system that was mounted on a van.[52]

[*] Once a 6-DoF model of parachute or parafoil has been developed, adding two or three DoF (depending on a specific joint) for payload is a relatively minor addition, which is quite similar for both parachutes or parafoils. More enhanced model may include the model of a joint (say elastic riser) itself allowing for more DoF.

The parachute-riser-payload system by Fallon was modeled as three bodies each with 6-DoF.[53] Since the parachute and payload were connected by the riser, and given the constraints of the riser, they reduced parachute-riser-payload system to a 15-DoF problem. Later, Doherr and Schilling reported on the development of a 9-DoF dynamic model of rotating parachutes which was used to decelerate and spin the submunitions of defense weapons.[54,55] This model described the parachute's behavior using Euler differential equations and payload's attitude using quaternions (to avoid singularities). It therefore included 19 (versus usual 18) independent variables. The differential equations were later converted to state-space representation by considering the apparent mass terms to be external forces and moments caused by accelerations and velocities at an earlier time (t-τ) (the time delay τ was derived from the earlier experimental observations during water tunnel tests). The stochastic disturbance was added to aerodynamic forces to address the issue of nonrigid nature of the parachute system. By comparing results from 6-DoF and 9-DoF models, they conclude a 9-DoF model predicts stability characteristics more adequately (realistically). Furthermore, their work established the very high sensitivity of the motion of a parachute-payload system to atmospheric disturbances.

Cockrell and Haidar considered the influence of canopy-payload coupling (accounting for added masses) on dynamic stability in pitch.[56] They used planar equations for two bodies (they refer to the earlier work by Frucht[57]). The paper by Moulin pointed out the importance of the modeling the link between the parachute and the load by showing its contribution to the dynamic behavior of this complex system.[58] An 8-DoF model was presented with its sensitivity to the driving parameters based on physical considerations. Vishnyak considered 12-DoF model of non-rigid parachute-payload system with elastic connection (they used quaternions for kinematics).[59]

Hailiang and Zizeng used a 9-DoF model to study motion of a parafoil and payload system.[60] In contrast to Doherr and Schilling, they reported only small differences in the motion and stability between 6-DoF and 9-DoF dynamic models. In studying stability characteristics as a function of the pitch inertia of the pay-load, Hailiang and Zizeng found the decay ratio and period increase as pitch inertia is increased.

The latest model of Wolf allowed 5 DoF for each body of the parachute-payload system, with roll about axisymmetry being neglected.[61] The major assumptions are rigid, axisymmetric parachute and payload bodies, flat earth with no wind. The model described motion of two dynamically coupled rigid bodies upon which simplified aerodynamic forces acted. Using this 10-DoF representation, Wolf established that stability is reduced as riser length is increased or parachute weight is increased and that stability is improved by increasing parachute axial and normal aerodynamic force. More recent efforts by Zhu *et al.* as well as Gupta *et al.* have incorporated parafoil structural dynamics into the dynamic model of a parachute and pay-load system.[47,62]

In support of future control system development Entchev *et al*. characterized the dynamics of a small parafoil (canopy and payload) as a 6-DoF nonlinear numerical simulation based on a rigid-body paradigm (aircraft EoM) and aerodynamic model of the system (23 static coefficients).[63] This simulation was based on construction of a scale rigid model of the canopy and wind tunnel testing of the same, CFD analysis, vehicle geometry measurements and mass properties estimation. The validity of the simulation was assessed using further CFD analysis and comparison with current parafoil theory. Sensitivity to various parameters was established and the accuracy of the rigid body approximation was assessed as quite satisfactory for further design of guidance, navigation and control (GNC) system for guided Airborne Delivery System (GPADS for the US Army Soldier System Command). Mortaloni *et al.* reported the development of a 6-DoF Simulink model of the Pegasus-500 parafoil-payload system by FXC Corporation.[10] Both diagonal and non-diagonal terms of the apparent mass matrix were taken into account. Model was tuned to perfectly match results of a real drop of the system. The complete model was later used for the design and simulation of the autonomous GNC system.

Slegers and Costello presented a model in which combined system of parafoil and payload was modeled with 9 DoF.[64] The model included three inertial position components of the joint (incorporating rotational stiffness and damping coefficients of joint) as well as the three Euler orientation angles for parafoil and payload. The model used apparent terms of Lissaman and Brown.[34] The parafoil's shape was modeled as a collection of joint panels (Fig.1) to address the issue of realistic initial disturbance while X-38 parafoil section-by-section opening. It was shown that for the small brake deflections parafoil-payload systems exhibit two modes of directional control: roll and skid steering. Although the model only employed basic aerodynamic coefficients, neglecting the majority of them, it could however simulate reasonable control response from both left and right deflection and parafoil tilt. Using a dynamic modeling approach similar to Doherr and Schilling and Hailiang and Zizeng, stability and control characteristics of this system were examined. Particular attention was paid to steady-state control response as a function of fundamental design parameters such as parafoil canopy geometry, angle of incidence, and varying control deflection.

Mooij *et al*. described detailed mathematical modeling of 9-DoF parafoil and payload system.[65] The parafoil system was modeled as a rigid parafoil and rigid store that were connected to each other by rigid suspension lines

and a riser. Included in the riser was a hinge that allowed free three axes rotation of the parafoil with respect to the store and it transfers only forces, but no moment. The hinge was modeled as a damped spring. The earth was assumed to be spherical and rotating to account for Coriolis and transportation acceleration.

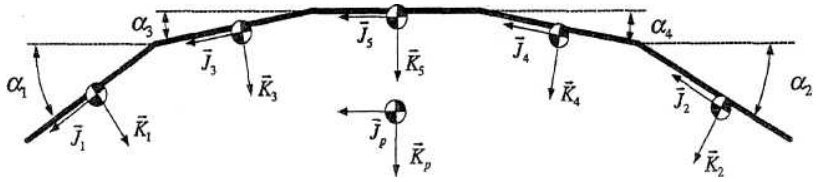

Figure 1. Parafoil canopy geometry used by Slegers and Costello.[64]

The latest work by Müller *et al.* described the highly-realistic 8-DoF model of the parafoil system.[66] It presented nonlinear differential equations of the system and included detailed simulations of dynamic reactions to symmetric and asymmetric control inputs, to atmospheric disturbances and to a twisted payload.

III. Identification and Scalability

As seen from the previous section, a variety of models of different parafoil-payload systems has been developed over past 40 years. The majority of them deals with simplified models addressing some specific issues. However, several higher-fidelity models have also been presented. By higher-fidelity we mean 6-DoF models considering parafoil-payload system as a rigid body, and higher DoF models considering a flexible joint between the parafoil and payload. Some of these joints allow pitching, rolling and yawing of the payload around the confluence point (joint) therefore adding 3 additional DoF. So in this case 9-DoF models are considered (alternatively one may say it is a 6-DoF model for the payload plus 3 DoF for parafoil with respect to the payload). If the joint restricts some of these motions (usually rolling) then it is lower than 9-DoF models (8-DoF for non-rolling joint). Introducing a joint or a suspension system (for instance having elastic suspension lines) as a separate subsystem obviously adds more DoF.

Some of the aerodynamic coefficients in these high-fidelity models are taken/extrapolated from aforementioned experimental wind-tunnel data (meaning they do not belong to the concrete system one tries to model) and/or CFD simulations (which are not complete and may be way off), some are simply neglected. Some papers provide results of flight tests and suggest how to extract and validate certain characteristics. The issue of apparent masses has also been addressed and empirical formulas for both diagonal and non-diagonal terms have been derived and used by many researchers in their models.

The models developed for different parafoil-payload systems behave well and produce reasonable transition behavior and integral performance, attesting quite a mature stage of such systems modeling. Therefore, one of the important issues to address now is not the development of the model itself (besides, EoM are well-known and initial guesses on the majority of the coefficients can be also obtained), but the technique capable of reliable and effective model identification with consecutive adjustment of initial-guess coefficients to better approximate real drop data. Recently, the scaling a parafoil-payload model (its coefficients and parameters) also became an important issue. (To our knowledge only Goodrick presented data and analysis of scale effects on ram-air parachutes based on his 6-DoF model simulations for parafoil wings areas from 32 to 6400ft^2 and for wing loadings from 1 to 4lb/ft^2.[67])

As mentioned in the previous section the variety of models higher than the point-mass models exists for both parafoil-payload systems:

- 9-DoF model by Hailiang and Zizeng;[60]
- 8-DoF model by Slegers and Costello;[64]
- 9-DoF model by Mooij *et al.*;[65]
- 8-DoF model by Müller *et al.*;[66]

and parachute-payload systems (the order of the model corresponds to that of claimed by the authors):

- 10-DoF model by Pillasch and Shen;[51]
- 9-DoF model by Reif;[52]
- 9-DoF model by Doherr and Schilling;[54,55]
- 8-DoF model by Moulin;[58]
- 12-DoF model by Vishnyak;[59]
- 15-DoF model by Fallon.[53]

Moreover, if the 6-DoF model of some system has been developed already, than adding additional degrees of freedom for the payload is a natural next step (the problem is not in adding two or three more degrees rather than in identification of such model since usually the only data recorded during the real drop is the data related to the payload). The EoM written for the center of gravity of the entire system (Fig.2a), should be rewritten for the parafoil and payload separately (Fig.2b) accommodating additional equations describing parafoil-payload coupling reactions for the concrete bundle (at the confluence point). So the previously developed and well-tested 6-DoF model of the Pegasus parafoil-payload system[10] was used as a basis for the scalable model development.

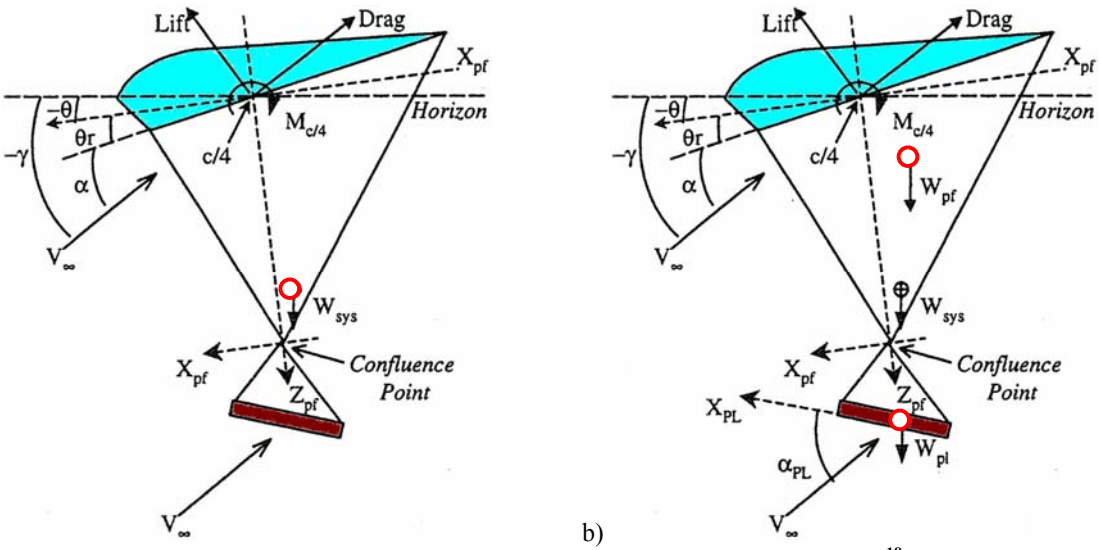

Figure 2. Rigid one-body system (a) versus flexible two-body system (b).[18]

In general the 8-DoF (9-DoF) model of the parafoil-payload system can be brought to the following sets dynamic and kinematic equations

$$\dot{\mathbf{V}}^{*T} = \mathbf{A}^{-1}\left\{\begin{bmatrix}\mathbf{F}\\ \mathbf{M}_c\\ \mathbf{M}_p\end{bmatrix} - \boldsymbol{\Sigma}\mathbf{A}\mathbf{V}^*\right\} \tag{1}$$

$$\dot{\boldsymbol{\Lambda}}_c = \tilde{\mathbf{R}}_E(\boldsymbol{\Lambda}_c)\boldsymbol{\omega}_c \tag{2}$$

$$\dot{\boldsymbol{\Lambda}}_p = \tilde{\mathbf{R}}_E(\boldsymbol{\Lambda}_p)\boldsymbol{\omega}_p \tag{3}$$

$$\dot{\mathbf{P}}_i = {}^i_b\mathbf{R}\mathbf{V}\,, \tag{4}$$

where vector $\mathbf{V}^* = \left[\mathbf{V}^T, \boldsymbol{\omega}_c^T, \boldsymbol{\omega}_p^T\right]^T$ consists of a velocity vector of the confluence point $\mathbf{V} = [u, v, w]^T$, angular velocity vectors of parafoil (canopy) $\boldsymbol{\omega}_c = [p_c, q_c, r_c]^T$ and payload $\boldsymbol{\omega}_p = [0, q_p, r_p]^T$, vectors $\boldsymbol{\Lambda}_c$ and $\boldsymbol{\Lambda}_c$ ($\boldsymbol{\Lambda} = [\varphi, \theta, \psi]^T$) constitute Euler angle triads for the canopy and payload respectively, $\mathbf{P}_i$ presents an inertial position of the system (confluence point). On the right-hand side of Eq.(1), block 3-by-3 matrix $\mathbf{A}$ (where each element is a 3-by-3 matrix itself) represents a mass-inertia matrix of the system, vectors $\mathbf{F}$, $\mathbf{M}_c$ and $\mathbf{M}_p$ constitute aerodynamic force and moment acting on the system and its two components (canopy and payload respectively), and matrix $\boldsymbol{\Sigma}$ is a block 3-by-3 matrix where each element is a 3-by-3 matrix too. In Eqs.(2),(3), notation $\tilde{\mathbf{R}}_E(\boldsymbol{\Lambda})$ stands for the matrix operator acting on a vector $\boldsymbol{\Lambda}$

$$\dot{\boldsymbol{\Lambda}} = \begin{bmatrix}1 & \sin\varphi\,\mathrm{tg}\theta & \cos\varphi\,\mathrm{tg}\theta\\ 0 & \cos\varphi & -\sin\varphi\\ 0 & \sin\varphi/\cos\theta & \cos\varphi/\cos\theta\end{bmatrix}\boldsymbol{\omega} = \tilde{\mathbf{R}}_E(\boldsymbol{\Lambda})\boldsymbol{\omega} \tag{5}$$

and matrix ${}^i_b\mathbf{R}$ in Eq.(4) is the rotation matrix

$$ {}^{i}_{b}\mathbf{R} = \begin{bmatrix} \cos\psi\cos\theta & \sin\psi\cos\theta & -\sin\theta \\ \cos\psi\sin\theta\sin\varphi\text{-}\sin\psi\cos\varphi & \sin\psi\sin\theta\sin\varphi+\cos\psi\cos\varphi & \cos\theta\sin\varphi \\ \cos\psi\sin\theta\cos\varphi+\sin\psi\sin\varphi & \sin\psi\sin\theta\cos\varphi\text{-}\cos\psi\sin\varphi & \cos\theta\cos\varphi \end{bmatrix}^{T} \tag{6} $$

Equation (1) (nine scalar equations) describes systems dynamics, while the rest of them (Eqs.(2)-(4)) – system's kinematics. If the opening stage is to be also considered than in order to avoid singularities it is worth substituting Eq.(3) with

$$ \dot{\mathbf{Q}}_p = \frac{1}{2}\begin{bmatrix} 0 & -\boldsymbol{\omega}_p^T \\ \boldsymbol{\omega}_p & -\mathbf{S}(\boldsymbol{\omega}_p) \end{bmatrix}\mathbf{Q}_p, \ \left\|\mathbf{Q}_p\right\| = 1 \tag{7} $$

(notation $\mathbf{S}(\boldsymbol{\xi}) = \begin{bmatrix} 0 & -\xi_3 & \xi_2 \\ \xi_3 & 0 & -\xi_1 \\ -\xi_2 & \xi_1 & 0 \end{bmatrix}$ for the skew matrices is used), applicable for quaternions

$$ \mathbf{Q}_p = \begin{bmatrix} q_0 \\ q_1 \\ q_2 \\ q_3 \end{bmatrix} = \begin{bmatrix} \cos\frac{\psi_p}{2}\cos\frac{\theta_p}{2}\cos\frac{\varphi_p}{2}+\sin\frac{\psi_p}{2}\sin\frac{\theta_p}{2}\sin\frac{\varphi_p}{2} \\ \cos\frac{\psi_p}{2}\cos\frac{\theta_p}{2}\sin\frac{\varphi_p}{2}-\sin\frac{\psi_p}{2}\sin\frac{\theta_p}{2}\cos\frac{\varphi_p}{2} \\ \cos\frac{\psi_p}{2}\sin\frac{\theta_p}{2}\cos\frac{\varphi_p}{2}+\sin\frac{\psi_p}{2}\cos\frac{\theta_p}{2}\sin\frac{\varphi_p}{2} \\ \sin\frac{\psi_p}{2}\cos\frac{\theta_p}{2}\cos\frac{\varphi_p}{2}-\cos\frac{\psi_p}{2}\sin\frac{\theta_p}{2}\sin\frac{\varphi_p}{2} \end{bmatrix} = \tilde{\mathbf{R}}_Q(\boldsymbol{\Lambda}_p) \tag{8} $$

(notation $\tilde{\mathbf{R}}_Q(\boldsymbol{\Lambda})$ stands for the matrix operator acting on a vector $\boldsymbol{\Lambda}$). The rotation matrix ${}^{i}_{b}\mathbf{R}$ in Eq.(4) in this case would be compound as

$$ {}^{i}_{b}\mathbf{R} = \begin{bmatrix} 1-2(q_2^2+q_3^2) & 2(q_1q_2+q_0q_3) & 2(q_1q_3-q_0q_2) \\ 2(q_2q_1-q_0q_3) & 1-2(q_3^2+q_1^2) & 2(q_2q_3+q_0q_1) \\ 2(q_3q_1+q_0q_2) & 2(q_3q_2-q_0q_1) & 1-2(q_1^2+q_2^2) \end{bmatrix}^{T}, \tag{9} $$

and the relationship between quaternions and Euler angles established by

$$ \boldsymbol{\Lambda}_p = \begin{bmatrix} \tan^{-1}\frac{2(q_2q_3+q_0q_1)}{1-2(q_1^2+q_2^2)} & -\sin^{-1}(2(q_1q_3-q_0q_2)) & \tan^{-1}\frac{2(q_1q_2+q_0q_3)}{1-2(q_2^2+q_3^2)} \end{bmatrix}^{T}. \tag{10} $$

The dependences of aerodynamic and control coefficients versus angle of attack were developed earlier based on the available data[13] tuned to match the flight test data.[10] Parafoil-payload coupling reactions were modeled in pretty much the same manner as say in Refs.54,55,66. (As expected at this time, not many changes were observed when the outputs of the 6-DoF and 8-DoF models were compared.)

Further attempts were devoted to the development of a scalable model assuming that the data from real drops of several different parafoil-payload systems becomes available. Although up until now only two incomplete sets of data for each of two systems shown on Fig.3 is available (both systems only differ by the way payload is attached) the following addresses some steps made to convert the model of a specific payload delivery system to that of general system requiring only limited amount of geometry/mass inputs.

Figure 3. Generic parafoil-payload system with different ways of payload attachment.

We assume first that nothing but just a single geometric parameter is known a priory. The goal then would be to determine the rest of them from observation of the descending system. To this end, Fig.4 shows an example of several front-view images of the system with superimposed theoretical skeleton.

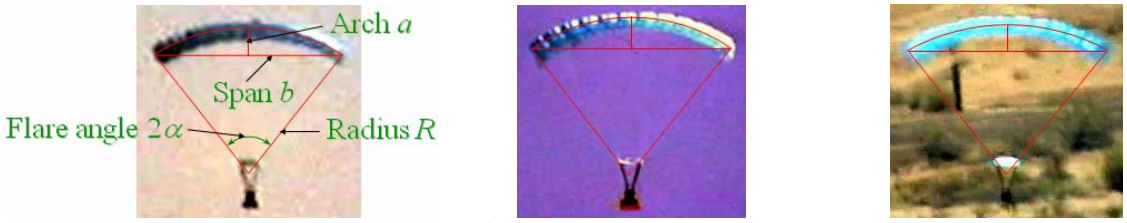

Figure 4. Front-view geometry.

For this skeleton the following theoretical dependences hold

$$\overline{R} = (2\alpha)^{-1}, \quad \overline{b} = 2\left(\overline{R} - \overline{a}\right)\mathrm{tg}\,\alpha, \quad \overline{b}^2 = 8\overline{R}^2\left(1 - \cos\alpha\right) - 4\overline{a}^2 \tag{11}$$

(here a bar denotes relative quantities related to the span of uninflated parafoil b_u). These dependences of front-view system parameters versus flare angle are shown on Fig.5. The values of the very same parameters as estimated from analyzing video data are also presented on Fig.5 demonstrating the perfect match. That means that by observing the flare angle with known span b_u the rest parameters (radius R, arch a, span b, arch-to-span ratio and front suspension line length) can be accurately estimated using Eqs.(11). The accuracy of the estimates can be found from Eq.(11) as

$$\frac{\delta R}{R} = -\frac{\delta\alpha}{\alpha}. \tag{12}$$

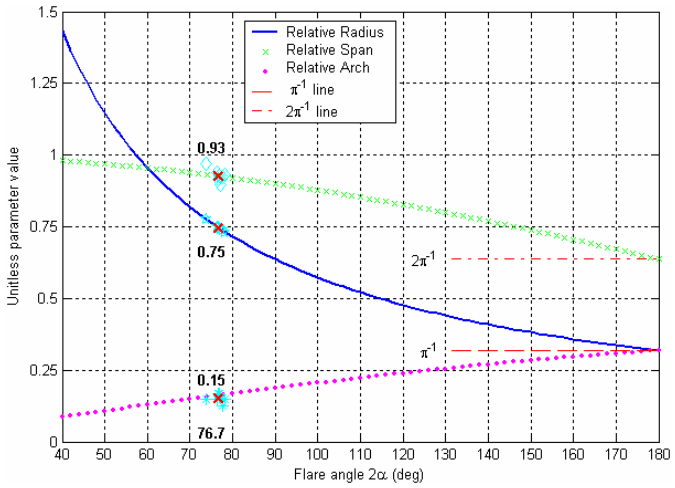

Figure 5. Dependences of relative front-view geometry parameters on the flare angle.

Proceeding with analyzing the side-view geometry of the system with now known radius R, it is possible to reconstruct the magnitude of a chord c, aspect ratio b/c and the geometry of the suspension system (Fig.6). As known the aspect ratio defines the parafoil aerodynamics, so that the nominal dependences of aerodynamic and control coefficients versus angle of attack (developed originally for the certain system with a certain aspect ratio) may now be adjusted by some empirical coefficients to be found during the following system identification stage.

Knowing the front- and side-view geometry also allows to proceed with the defining a location of the center of gravity (CG) of the airfoil and inflated parafoil (assuming the circular model, center of gravity of the inflated parafoil lies $R\left(1 - \dfrac{\sin\alpha}{\alpha}\right)$ beneath the CG of the airfoil along the line tilted clockwise by the rigging angle) as well with the estimating parafoil and entrapped air masses (Fig.7).

The following step would be adding payload data and defining the type of a joint to adjust coupling reactions between parafoil and payload.

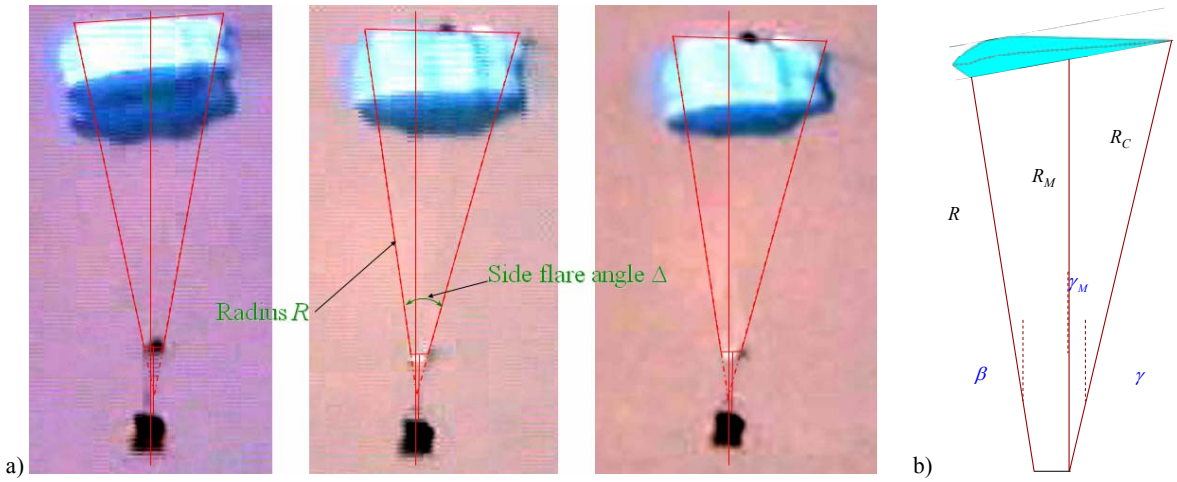

Figure 6. Side-view geometry (a) and geometry of the suspension system (b).

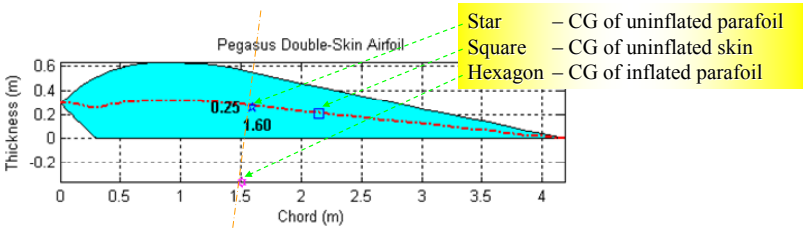

Figure 7. Side-view geometry of the airfoil.

The set of variable gains was introduced to address the model identification/scalability issue. This set includes a group of aerodynamic force coefficients $\mathbf{k}_F$, a group of moment coefficients $\mathbf{k}_M$, a group of mass-geometry coefficients $\mathbf{k}_G$, and a group of apparent mass coefficients $\mathbf{k}_\alpha$. The total number of these coefficients exceeds several dozens. Nominally, for the original model these coefficients or gains are equal to unity. The goal of the following identification is to adjust these coefficients so that they provide the best match between simulations and real drop data for several different parafoil-payload systems simultaneously. In such a case the defined gains would constitute a generic parafoil-payload system model allowing to use it as an initial guess when designing a brand new system (when only a few basic parameters are known). Of course later the model may be adjusted further to match the real drop data of this specific system rather than some generalized system.

Figure 8 presents the hierarchy and the task flow of the developed software.

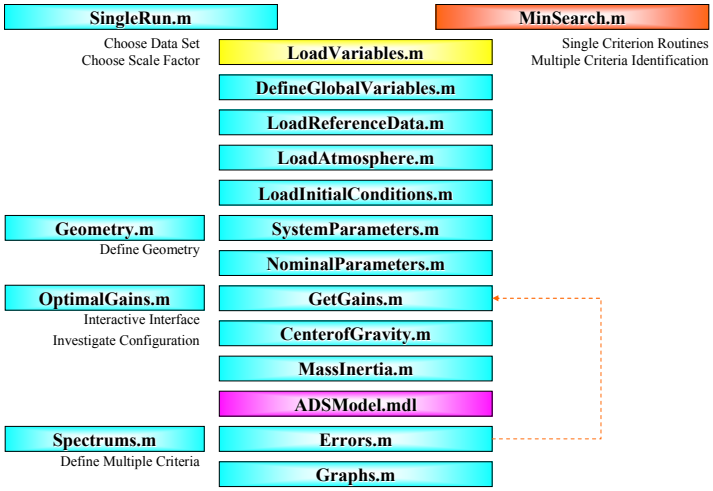

Figure 8. Software architecture.

The core element in this hierarchy is the Simulink model of the system itself (*ADSMODEL.mdl* on Fig.8). But before this system can be run, all input parameters should be supplied (by default the nominal Pegasus system is considered). If the real drop data is available than identification routine may be employed. In more general case when almost nothing is known yet for sure, multiparameter multicriteria software is used.[11] If there is a need to adjust just a few parameters rather than dozens of them, than a simple single-criterion method can be employed. Figure 9 shows that during identification (or after it) any variable gain may be interactively changed directly that gives the developed tool sort of flexibility from one the hand and the way to explore the influence of a certain parameter from the other hand.

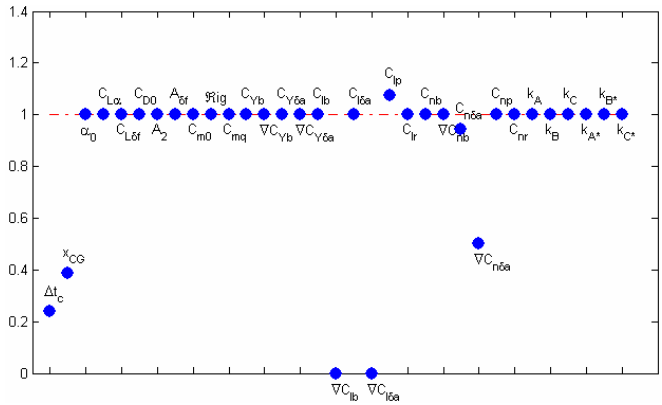

Figure 9. Interactive interface for variable gains.

IV. Conclusion

The paper describes the previous efforts in modeling different parafoil-based payload delivery systems and in obtaining aerodynamic and control coefficients for the parafoil itself. Based on the available wind-tunnel data for different parafoils and recent successes in the development and validation of the high-fidelity models of several similar parafoil-payload systems, the efforts have been made to convert the 6-DoF model developed earlier for a specific parafoil-payload system to a higher-degree-of-freedom model capable to be tuned to another system, meaning capable to be scaled. Several dozens of variable gains were introduced to allow this capability. While the paper presents a current status of development of correspondent software to address the issue of model identification and scalability, the author hopes to use this software to proceed with a scalable high-fidelity model of the generic parafoil-payload system in the nearest future when more experimental data becomes available.

References

[1] Nicolaides, J.D., Knapp, C.F., "A Preliminary Study of the Aerodynamic and Flight Performance of the Parafoil," AIAA Paper 1965, *1st AIAA Conference on Aerodynamic Decelerator Systems*, University of Minnesota, MN, July 8, 1965.

[2] Nicolaides, J.D., "On the Discovery and Research of the Parafoil," *International Congress on Air Technology*, Little Rock, AK, 1965.

[3] Knapp, C.F., Barton, W.R., "Controlled recovery of Payloads at Large Glide Distances, Using the Para-Foil," Journal of Aircraft, 5(**2**), 1968.

[4] Nicolaides, J.D., Speelman, R.J., Menard, G.L.C., "A Review of Para-Foil Programs," AIAA Paper 1968, *2nd AIAA ADS Conference*, El Centro, CA, September 23-25, 1968.

[5] Nicolaides, J.D., "Improved Aeronautical Efficiency Through Packable Weightless Wings," AIAA Paper 1970-880, *CASI/AIAA Meeting on the Prospects for Improvement in Efficiency of Flight*, Toronto, Canada, July 9-10, 1970.

[6] Nicolaides, J.D., Speelman, R.J., Menard, G.L.C., "A Review of Para-Foil Applications," *Journal of Aircraft*, 7(**5**), 1970.

[7] Nicolaides, J.D., Tragarz, M.A., "Parafoil flight performance," AIAA Paper 1970-1190, *3rd AIAA ADS Conference*, Dayton, OH, September, 14-16, 1970.

[8] Lingard, J.S., "The Performance and Design of Ram-Air Parachutes," TR-81-103, UK Royal Aircraft Establishment, Farnborough, 1981.

[9] Poynter, D., The Parachute Manual. A Technical Treatise on Aerodynamic Decelerators, Vol.2, 1991.

[10] Mortaloni, P., Yakimenko, O., Dobrokhodov, V., and Howard, R., "On the Development of a Six-Degree-of-Freedom Model of a Low-Aspect-Ratio Parafoil Delivery System," *17th AIAA Aerodynamic Decelerator Systems Technology Conference and Seminar*, Monterey, CA, May 19-22, 2003.

[11] Yakimenko, O.A., Statnikov, R.B., "Multicriteria Parametrical Identification of the Parafoil-Load Delivery System," *Proc. of the 18th AIAA Aerodynamic Decelerator Systems Technology Conference*, Munich, Germany, May 24-26, 2005.

[12] Burk, S.M., Ware, G.M., Static Aerodynamic Characteristics of Three Ram-Air Inflated Low Aspect Ratio Fabric Wings, TN-D-4182, NASA, 1967.

[13] Ware, G.M., Hassell, J.L., Jr., Wind-Tunnel Investigation of Ram-Air-Inflated All-Flexible Wings of Aspect Ratios 1.0 to 3.0, TM SX-1923, NASA Langley Research Center, Hampton, VA, 1969.

[14] Wailes, W.K., "Advanced Recovery Systems for Advanced Launch Vehicles (ARS). Phase 1 Study Results," AIAA Paper 1989-0881, *10th AIAA ADST Conference*, Cocoa Beach, FL, April 18-20, 1989.

[15] Wailes, W.K., "Development testing of large ram air inflated wings," AIAA Paper 1993-1204, *12th RAeS/AIAA ADST Conference and Seminar*, London, England, May 10-13, 1993.

[16] Geiger, R.H., Wailes, W.K., "Advanced Recovery Systems Wind Tunnel Test Report," CR-177563, NASA Ames Research Center, Pioneer Aerospace Corporation, Melbourne, FL, August 1990.

[17] Iacomini C.S., Cerimele C.J., "Lateral-directional aerodynamics from a large scale parafoil test program," AIAA Paper 1999-1731, *15th CEAS/AIAA ADST Conference*, Toulouse, France, June 8-11, 1999.

[18] Iacomini C.S., Cerimele C.J., "Longitudinal aerodynamics from a large scale parafoil test program," AIAA Paper 1999-1732, *15th CEAS/AIAA ADST Conference*, Toulouse, France, June 8-11, 1999.

[19] Iacomini C.S., Madsen, C.M., "Investigation of large scale parafoil rigging angles - Analytical and drop test results," AIAA Paper 1999-1752, *15th CEAS/AIAA ADST Conference*, Toulouse, France, June 8-11, 1999.

[20] Martin, F.W., Jr., "Parafoil Aerodynamic Characteristics Derived from Flight Measured Suspension Loads," AIAA Paper 1999-1734, *15th CEAS/AIAA ADST Conference*, Toulouse, France, June 8-11, 1999.

[21] Madsen, C.M., Cerimele C.J., "Updated flight performance and aerodynamics from a large scale parafoil test program," AIAA Paper 2000-4311, *AIAA MST Conference*, Denver, CO, August 14-17, 2000.

[22] Machin, R.A., Iacomini, C.S., Cerimele, C.J., Stein, J.M., "Flight testing the parachute system for the space station crew return vehicle," *Journal of Aircraft*, 38(**5**), 2001.

[23] Madsen, C.M., Cerimele C.J., "Flight performance, aerodynamics, and simulation development for the X-38 parafoil test program," AIAA Paper 2003-2108, *17th AIAA ADST Conference and Seminar*, Monterey, CA, May 19-22, 2003

[24] Lingard J.S., "The Aerodynamics of Gliding Parachutes," AIAA Paper 1986-2427, *9th Aerodynamic Decelerator and Balloon Technology Conference*, Albuquerque, October 7-91986.

[25] Goodrick, T.F., "Theoretical study of the longitudinal stability of high-performance gliding airdrop systems," AIAA Paper 1975-1394, *5th AIAA ADS Conference*, Albuquerque, NM, November 17-19, 1975.

[26] Goodrick, T.F., "Simulation studies of the flight dynamics of gliding parachute systems," AIAA Paper 1979-0417, *6th AIAA AD and Balloon Technology Conference*, Houston, TX, March 5-7, 1979.

[27] Goodrick, T.F., "Comparison of simulation and experimental data for a gliding parachute in dynamic flight," AIAA Paper 1981-1924, *7th AIAA ADBT Conference*, San Diego, CA, October 21-23, 1981.

[28] Crimi, P., "Lateral Stability of Gliding Parachutes," Journal of Guidance, Control Dynamics, 13(6), 1990.

[29] Iosilevskii, G., "Center of Gravity and Minimal Lift Coefficient Limits of a Gliding Parachute," Journal of Aircraft, 32(6), 1995, pp.1297-1302.

[30] Jann, T., "Aerodynamic model identification and GNC design for the parafoil-load system ALEX," AIAA Paper 2001-2015, *16th AIAA ADST Conference and Seminar*, Boston, MA, May 21-24, 2001.

[31] Schroeder, C., "Parafoil Dynamic Simulator," NASA Johnson Space Center, Nov. 1997.

[32] Prakash, O., Aerodynamics and Longitudinal Stability of Parafoil/Payload System, Preliminary Report 03401005, Department of Aerospace Engineering, Indian Institute of Technology, Bombay, May 2004.

[33] Cockrell, D.J., "Apparent mass - Its history and its engineering legacy for parachute aerodynamics," AIAA Paper 1991-0827, *11th AIAA ADST Conference*, Baltimore, MD, April 9-11, 1991.

[34] Lissaman, P.B.S., Brown, G.J., "Apparent mass effects on parafoil dynamics," AIAA Paper 1993-1236, *12th RAeS/AIAA ADS Technology Conference*, London, England, May 10-13, 1993.

[35] Brown, G. L, "Parafoil Steady Turn Response to Control Input," AIAA Paper 1993-1241, *12th RAeS/AIAA ADS Technology Conference*, London, England, May 10-13, 1993.

[36] Thomasson, P.G., "Equation of Motion of an Aircraft," *Journal of Aircraft*, 37(**4**), 2000, pp.630-639.

[37] Barrows, T.M., "Apparent mass of parafoils with spanwise camber," AIAA Paper 2001-2006, *16th AIAA ADST Conference and Seminar*, Boston, MA, May 21-24, 2001.

[38] Barrows, T.M., "Apparent mass of parafoils with spanwise camber," *Journal of Aircraft*, 39(**3**), 2002.

[39] Doherr, K.-F., Jann, T., "Test vehicle ALEX-I for low-cost autonomous parafoil landing experiments," AIAA Paper 1997-1543, *14th AIAA ADST Conference*, San Francisco, CA, June 3-5, 1997.

[40] Jann, T., Doherr, K.-F., Gockel W., "Parafoil test vehicle ALEX - Further development and flight test results," AIAA Paper 1999-1751, *15th CEAS/AIAA ADST Conference*, Toulouse, France, June 8-11, 1999.

[41] Tsai, H.B., Meiners, M.A., Lahr, E.K., "Analytical and Experimental Study of a Recovery Guidance System at Iowa State University," Iowa State University of Science and Technology, Ames, IA, 1999.

[42] Sego, W.K, Jr., "Development of a high glide, autonomous aerial delivery system - 'Pegasus 500 (APADS)," AIAA Paper 2001-2073, *16th AIAA ADST Conference and Seminar*, Boston, MA, May 21-24, 2001.

[43] Gonzales, M.A., "Prandtl Theory Applied to Paraglider Aerodynamics," AIAA Paper 1993-1220, *12th RAeS/AIAA ADST Conference and Seminar*, London, England, May 10-13, 1993.

[44] Iosilevskii, G.A., "Paraglider - Performance, Aerodynamics and Flight Mechanics," TAE-Report 692, Technion - Israel Institute of Technology, Faculty of Aerospace Engineering, 1993.

[45] Ross, J.C., "Computational Aerodynamics in the Design and Analysis of Ram-Air Inflated Wings," AIAA Paper 1993-1228, *12th RAeS/AIAA ADST Conference and Seminar*, London, England, May 10-13, 1993.

[46] Mosseev, Yu., "Software tools for the paraglider computer-aided design guide," AIAA Paper 2001-2001, *16th AIAA ADST Conference and Seminar*, Boston, MA, May 21-24, 2001.

[47] Zhu, Y., Moreau, M., Accorsi, M., Leonard, J., and Smith, J., "Computer Simulation of Parafoil Dynamics," AIAA Paper 2001-2005, *16th AIAA ADST Conference and Seminar*, Boston, MA, May 21-24, 2001.

[48] Jann, T., "Aerodynamic coefficients for a parafoil wing with arc anhedral - theoretical and experimental results," AIAA Paper 2003-2106, *17th AIAA ADST Conference and Seminar*, Monterey, CA, May 19-22, 2003.

[49] Kroo, I., "LinAir for the Macintosh," Desktop Aeronautics, 1987 (P.O. Box 9937, Stanford, CA 94305).

[50] Wolf D.F., "A Coupling Apparent Mass for Parachute Inflation Equations," AIAA Paper 1989-0933, *10th AIAA ADST Conference*, Cocoa Beach, FL, April 18-20, 1989.

[51] Pillasch, D. W.Shen, Y.C., Valero, N., "Parachute/Submunition System Coupled Dynamics," AIAA Paper 1984-0784, *8th AIAA ADBT Conference*, Hyannis, MA, April 2-4, 1984.

[52] Reif, J., Development of Parachutes for Weapon Applications in CCG – UofM, Course F12.01 on "Parachute Systems Technology; Fundamentals, Concepts and Applications," Oberpfaffenhofen, 22-26 June 1987.

[53] Fallon, E.J., "Parachute dynamics and stability analysis of the Queen Match Recovery System," AIAA Paper 1991-0879, *11th AIAA ADST Conference*, Baltimore, MD, April 9-11, 1991.

[54] Doherr, K.-F., Schilling, H., "9DOF-simulation of rotating parachute systems," AIAA Paper 1991-0877, *11th AIAA ADST Conference*, Baltimore, MD, April 9-11, 1991.

[55] Doherr, K.-F., Schilling, H., "Nine-degree-of-freedom simulation of rotating parachute systems," *Journal of Aircraft*, 29(**5**), 1992.

[56] Cockrell, D.J., Haidar, N.I.A., "Influence of the canopy-payload coupling on the dynamic stability in pitch of a parachute system," AIAA Paper 1993-1248, *12th RAeS/AIAA ADS Technology Conference*, London, England, May 10-13, 1993.

[57] Frucht, Y.I., "A Model for Simulating the Planar Motion of a Frictionless, Pin-Jointed Parachute-Payload System," University of Leicester Engineering Department Internal Report, March 1988.

[58] Moulin, J., "Recovery system simulation: Link modelization," AIAA Paper 1993-1249, *12th RAeS AIAA ADST Conference and Seminar*, London, England, May 10-13, 1993.

[59] Vishnyak, A., "Simulation of the payload-parachute-wing system flight dynamics," AIAA Paper 1993-1250, *12th RAeS/AIAA ADST Conference and Seminar*, London, England, May 10-13, 1993.

[60] Hailiang, M., and Zizeng, Q., "9-DoF Simulation of Controllable Parafoil System for Gliding and Stability," Journal of National University of Defense Technology, 16(**2**), 1994, pp.49-54.

[61] Wolf, D.F., "Parachute opening shock," AIAA Paper 1999-1702, *15th CEAS/AIAA ADST Conference*, Toulouse, France, June 8-11, 1999.

[62] Gupta, M., Xu, Z., Zhang, W., Accorsi, M., Leonard, J., Benney, R., and Stein, K., "Recent Advances in Structural Modeling of Parachute Dynamics," AIAA Paper 2001 -2030, *16th AIAA ADST Conference and Seminar*, Boston, MA, May 21-24, 2001.

[63] Entchev, R.O., Rubenstein, D., Modeling Small Parafoil Dynamics, Final Report 16.622, Spring 2001.

[64] Slegers, N., Costello, M., "Aspects of control for a parafoil and payload system," *Journal of Guidance, Control Dynamics*, 26(**6**), 2003.

[65] Mooij, E., Wijnands, Q. G. J., and Schat, B., "9 DoF Parafoil/Payload Simulator Development and Validation," *AIAA Modeling and Simulation Technologies Conference*, Austin, Texas, August 2003.

[66] Müller, S., Wagner O., Sachs, G., "A high-fidelity nonlinear multibody simulation model for parafoil systems," AIAA Paper 2003-2120, *17th AIAA ADST Conference and Seminar*, Monterey, CA, May 19-22, 2003.

[67] Goodrick, T.F., "Scale effects on performance of ram air wings," AIAA Paper 1984-0783, *8th AIAA ADBT Conference*, Hyannis, MA, April 2-4, 1984.